Preclinical evaluation and structural optimization of anti-BCMA CAR to target multiple myeloma

Ortal Harush,[1]* Nathalie Asherie,[2]* Shlomit Kfir-Erenfeld,[2]* Galit Adler,[1] Tilda Barliya,[1] Miri Assayag,[2] Moshe E. Gatt,[3] Polina Stepensky[2] and Cyrille J. Cohen[1]

[1]Laboratory of Tumor Immunology and Immunotherapy, The Mina and Everard Goodman Faculty of Life Sciences, Bar-Ilan University, Ramat Gan; [2]Department of Bone Marrow Transplantation and Cancer Immunotherapy, Hadassah Medical Center, Faculty of Medicine, Hebrew University of Jerusalem, Jerusalem and [3]Department of Hematology, Hadassah Medical Center, Faculty of Medicine, Hebrew University of Jerusalem, Jerusalem, Israel

*OH, NA and SKE contributed equally as co-first authors.

Abstract

Chimeric antigen receptor (CAR) T-cell based immunotherapy has become a promising treatment mainly for hematological malignancies. Following the major success of CD19-targeted CAR, new potential targets for other malignancies are required. As such, B-cell maturation antigen (BCMA) is an attractive tumor-associated antigen to be targeted in multiple myeloma (MM). Herein, we aimed at assessing the function and optimal configuration of different BCMA-specific CAR, based on the same targeting moiety but with a different hinge and co-stimulatory domain. We compared their function to that of a previously characterized BCMA-CAR used in clinical trials. All constructs were expressed at high levels by primary human T cells and could trigger cytokine production and cytotoxicity upon co-culture with multiple myeloma targets. Nonetheless, critical differences were observed in off-target activation, exhaustion, and activation marker expression and *in vivo* anti-tumoral activity mediated by these different constructs. Interestingly, we noted that CD8-based hinge, combined with a 4-1BB intracellular domain, proved superior compared to IgG4-connecting regions, and/or a CD28-signaling moiety respectively. Overall, this study emphasizes the influence of CAR primary structure on its function and led to the identification of a highly efficient BCMA-specific CAR, namely H8BB, which displayed superior anti-tumoral activity both *in vitro* and long-term *in vivo* efficacy.

Introduction

Multiple myeloma (MM) develops in the bone marrow by clonal expansion of malignant plasma cells and is associated with excessive production of monoclonal immunoglobulins in blood and urine.[1,2] Despite significant progress achieved in the treatment of MM, this disease remains incurable with a poor prognosis in relapsed/refractory (R/R) patients. Therefore, the development of novel therapeutic approaches to target MM is essential. Following the major success of CD19-targeted chimeric antigen receptor (CAR) therapy to hematological malignancies and its Food and Drug Administration (FDA) approval in 2017, new potential targets for CAR therapy are required.[3] In this regard, B-cell maturation antigen (BCMA) is a cell-surface protein belonging to the tumor necrosis factor receptor superfamily which promotes B-cell survival and proliferation.[4] Besides mature B-lymphocytes and plasma cells, BCMA is highly expressed in most cases of MM, making it an attractive target for CAR therapy.[5,6]

Kochenderfer and colleagues tested an anti-BCMA CAR in a clinical trial which resulted in 20% objective response rate (ORR) in the patient group treated with 0.3-3x10^{6} CAR-T cells/kg.[7] A higher ORR (81%) was achieved when using a higher dose (9x10^{6} cells/kg).[8,9] Several recent trials demonstrate the potential of anti-BCMA CAR approach in promising phase I/II studies, reaching up to 80% ORR with deep and durable responses in heavily pretreated patients with R/R multiple myeloma.[10-16] Based on the encouraging results of a phase II trial,[15] the FDA and European Medicines Agency approved Idecabtagene-Vicleucel (Ide-cel or bb2121) for the treatment of R/R MM patients. Another CAR-T-cell product, Ciltacabtagene-autoleucel (Cilta-cel), incorporates two anti-BCMA single heavy-chain domains

and a 4-1BB co-stimulatory domain, demonstrated an ORR over 97% without excessive toxicity in terms of cytokine release syndrome or neurotoxicity.[16]

CAR consist of two essential moieties: an extracellular binding domain and a signaling domain. The first is usually composed of a single-chain fragment variable (scFv) targeting a designed antigen, whereas the signaling domain, usually composed of co-stimulatory moiety (e.g., CD28 and/or 4-1BB), along with CD3ζ, facilitates T-cell activation. The type of co-stimulation can greatly facilitate CAR-T-cell persistence and metabolic activity (like in 4-1BB-based CAR), while CD28 promotes more potent but short-lived responses.[17] Connecting both CAR moieties, the hinge and transmembrane domains provide proper linkage and flexibility, influencing CAR-T-cell function, stability, and expression.[18,19] CAR hinge domain is often chosen according to the target ligand proximity to the cell membrane[20-22] and CAR structure must be optimized empirically to enhance its function. Moreover, a recent retrospective analysis of anti-CD19 CAR-T-based clinical studies further supports the idea that the structural composition of CAR domains, beyond scFv and co-stimulatory moieties, impacts clinical outcomes and related toxicities.[23]

Thus, we hypothesized that modifications in the primary structure of an originally described BCMA-specific CAR (referred to as "H828" herein) would improve its function.[7] In order to assess this, we constructed three novel anti-BCMA CAR and compared their function to that of H828. We performed extensive analysis of expression, cytokine production and cytotoxicity against myeloma cells while focusing also on "off-target", activation and exhaustion profiles, and on the *in vivo* efficacy of CAR-T cells. Our findings exemplify the contribution of different domains (i.e., hinge, TM and co-stimulatory portions) on CAR specificity and function, which may bear important implications for its implementation in clinical settings.

Methods

Peripheral blood mononuclear cells, bone marrow-derived manonuclear cells and cell lines

Peripheral blood mononuclear cells (PBMC) were from healthy donors obtained from the Israeli Blood Bank (Tel-Hashomer, Israel), the Pheresis Collection Unit, (IRB-approval #0458-19-HMO) or from blood of patients with plasma cell malignancies (IRB-approval #0253-20-HMO). BCMA+ cell lines are RPMI8226(ATCC/CCL-155), (NCI)-H929(ATCC/CRL-9068) and MM1.S(ATCC/CRL-2974). K562(ATCC/CCL-243) is an erythroleukemia line BCMA[neg]. K562-BCMA was engineered to overexpress BCMA. Cell lines were cultured in RPMI medium (Invitrogen, Carlsbad, CA), with 10% heat-inactivated fetal bovine serum (Biological Industries, Israel), at

37°C and 5% CO_2. Bone marrow (BM) aspirates from patients with plasma cell dyscrasias were obtained in accordance with Helsinki approval from the Ethical Committee of Hadassah Ein-Kerem Medical Center. BM-derived mononuclear cells were isolated by centrifugation over a density gradient medium (lymphocyte separation medium, Lonza). Lymphocytes were cultured in BioTarget medium (Biological Industries, Israel) with 10% fetal bovine serum, 1% L-glutamine, 1% penicilin/streptomycin and 300 IU/mL IL-2 (Peprotech-Asia, Israel).[24-26]

Anti-BCMA chimeric receptors

ICBB, IC28 and H8BB (Figure 1A) were created by overlapping polymerase chain reaction (PCR) based on the heavy chain followed by the light chain derived from the previously described C11D5.3 antibody.[7] ICBB and IC28 incorporated an optimized short IgG4-derived spacer and a Strep Tag[27], while H828 and H8BB incorporated CD8α-derived hinge and TM. The H828-CAR was a kind gift from Dr. Kochenderfer, NCI, NIH.[7] These chimeras were subcloned into the retroviral backbone pMSGV1 (a kind gift from Dr Steven Rosenberg, NCI). Retroviral transduction, co-cultures, enzyme-linked immunosorbant assay (ELISA) and cytotoxicity assays were performed as previously described.[28-30]

T-cell exhaustion/activation following antigen stimulation

CAR-T cells were co-cultured with target cells IL-2 medium overnight at an effector to target (E:T) ratio of 10:1, in T-cell medium without IL-2 and incubated for 24 hours at 37°C. Cells were stained with the indicated antibodies and analyzed by flow cytometry, gated on BCMA-CAR+.

Established tumor assay

Six to 12 week-old NOD/SCID/Gamma mice were subcutaneously injected with 4x10^{6} NCI H929 cells resuspended in 100 μL HBSS medium (Biological Industries, Beth Haemek, Israel) and 100 μL Cultrex matrix (Trevigen, MD). Transduced lymphocytes resuspended in 200 μL HBSS medium were injected after tumor inoculation. Tumor size was measured every 2-3 days using a caliper in a blinded fashion or assessed by injecting luciferin solution (5 mg/ml, 200 μLmouse, Promega) and bioluminescence imaging (BLI) evaluation. Animals were humanely euthanized if the tumor exceeded 16 mm in diameter. All the procedures were performed according to the guidelines of the University Committee for Animal Welfare.

Immunohistochemistry

Four micron-thick formalin-fixed paraffin-embedded (FFPE) tumor sections were stained with the anti-human CD3 antibody (103A-76/1507011D, CellMarque, 1:1,000), on
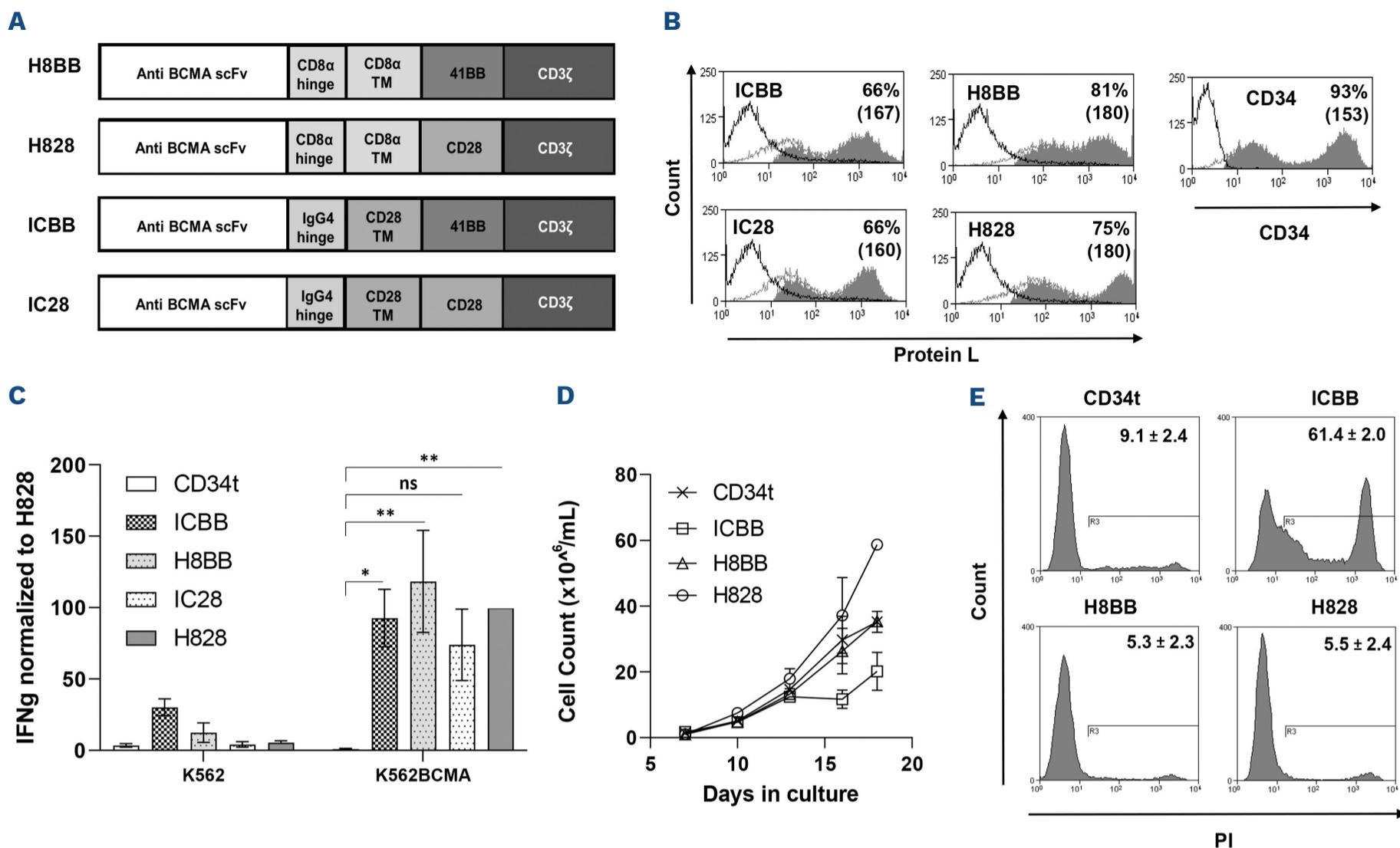
Figure 1. Characterization of anti-BCMA based chimeras. (A) Schematic representation of the different designs of anti-BCMA chimeric receptors described in the Materials and Methods section. (B) Anti-CD3-activated human primary peripheral blood mononuclear cells (PBMC) were transduced with the different anti-BCMA chimeric antigen receptor (CAR) or with truncated CD34 (CD34t, control gene), as indicated. These cells were stained using Protein L or anti-CD34 antibody, respectively. Transgene expression was assessed by flow cytometry. The dotted line represents the staining of the mock-transduced control cells. The percentage of positive cells and the mean fluorescence intensity (MFI) (in brackets) are shown. The graph represents the average of 4 different donors and the difference in the staining between the population transduced with BCMA-CAR and the control population was found statistically significant ($P<0.05$; calculated using a Student's paired *t*-test). (C) Co-culture of 1e5 transduced cells with 1e5 K562-BCMA or K562 cells (negative control) for 16 hours. Interferon γ (IFNγ) secreted in the co-culture supernatant was measured by enzyme-linked immunosorbant assay. These results are representative of 3 independent experiments. (D) Cell concentration was determined for BCMA-CAR-T cells and control T cells every 2-3 days for 3 weeks. These results are representative of 3 independent experiments with different donors (ICBB *vs.* H8BB/H828, $P<0.05$; by two-way ANOVA). (D) Cell viability was assessed 3 weeks following transduction. BCMA-CAR T cells were stained with propidium iodide (PI) and analyzed by flow cytometry, ICBB *vs.* H8BB/H828, $P<0.001$, by paired Student's *t*-test. BCMA: B-cell maturation antigen.

a BenchMark ULTRA-autostainer (Ventana Medical Systems) with standard antigen retrieval (CC1-buffer, 40 minutes). Detection was performed using the ultraView Universal-DAB Detection-Kit (Ventana Medical Systems).

Statistical analysis

Statistical analyses were performed using GraphPad Prism (V9.1.0). Unless otherwise stated, paired Student's *t*-test or two-way ANOVA tests were used for normal data at equal variance. $P<0.05$ was considered significant and is marked as * in the figures. T cells from at least three different healthy donors were used for all *in vitro* and *in vivo* experiments. Kruskal-Wallis analysis with Dunn's *post hoc* analysis was performed for mouse tumor volumes. Analysis of variance or log-rank (Mantel-Cox) test for survival data were performed.

Results

Generation of different anti-BCMA CAR and preliminary evaluation

Herein, we designed and constructed three second-generation anti-BCMA CAR based on the heavy and light chains derived from the C11D5.3 antibody.[7] As co-stimulatory molecules, these CAR incorporate either an intracellular domain derived from 4-1BB (for H8BB and ICBB) or CD28 (for IC28) (Figure 1A). More specifically, H8BB includes hinge and transmembrane (TM) domains derived from CD8α, while these were replaced by an IgG4 hinge and a CD28 TM in the ICBB. IC28 shares the same hinge and CD28 TM domain as ICBB, but its co-stimulatory domain was switched from 4-1BB to CD28 (Figure 1A). As a reference, we used the previously described[7] and clinically

tested[8] H828 CAR (also based on the C11D5.3 antibody), which incorporates a CD8α-derived hinge-TM and CD28 as co-stimulatory domain.

We then evaluated the function of the BCMA-specific CAR. To that end, anti-CD3-stimulated human PBMC were transduced with these different CAR. As shown in Figure 1B, BCMA CAR molecules were expressed at high levels, ranging from 66% for ICBB to 81% for H8BB. We performed an overnight co-culture of CAR-transduced T cells with target cells (K562 *vs.* K562-BCMA) and measured IFNγ secretion by ELISA. All four anti-BCMA CAR mediated IFNγ release (Figure 1C). Yet, although IC28 could induce cytokine release upon specific stimuli, it was less efficient than the other CAR in mediating cytokine release (Figure 1C, IC28 *vs.* CD34t, ns), in killing assays and at upregulating activation markers upon antigen stimulation (data not shown). Additionally, H8BB CAR-T cells secreted less IFNγ than corresponding ICBB CAR-T cells (*P*<0.05) in the presence of the BCMA-negative control cell line K562. Since both chimeras share the same scFv and co-stimulatory domains, this observation may indicate that the hinge and TM moieties incorporated into these CAR may affect their "off-target" specificity. Given these preliminary data and based on emerging studies demonstrating 4-1BB co-stimulation benefits,[17,31] we decided to focus on 4-1BB-based CAR, namely ICBB and H8BB.

Growth and viability of T cells transduced with the different anti-BCMA chimeras

Next, we monitored the growth of the different BCMA CAR-transduced T cells over 18 days of culture. Figure 1D shows that ICBB CAR-T cells display the slowest expansion profile (ICBB *vs.* H8BB/H828/CD34t, *P*<0.05). Additionally, we assessed BCMA-CAR T-cell viability with propidium iodide (PI) staining. Figure 1E indicates that a large proportion of ICBB-transduced cells were positive for PI (61.4±2.0%) compared to the other groups (5.3-9.1%; *P*<0.0001). This indicates that H8BB-transduced cells have a similar ability to expand *in vitro* over time as H828-transduced cells, while ICBB-transduced cells exhibit an increased cell death (Figure 1E) and a subsequent reduced ability to expand (Figure 1D).

Cytokine secretion by BCMA-specific CAR

Following our initial evaluation of CAR functionality, we conducted wider cytokine secretion assays by co-culturing BCMA-CAR-transduced T cells with different plasma and MM cell lines. In general, BCMA CAR T-cells could specifically secrete high levels of cytokines (IFNγ, TNFα and IL-2) important for anti-tumor immunity,[32] when compared to CD34t negative control CAR-T cells (Figure 2; *P*<0.05). More precisely, in co-cultures with target
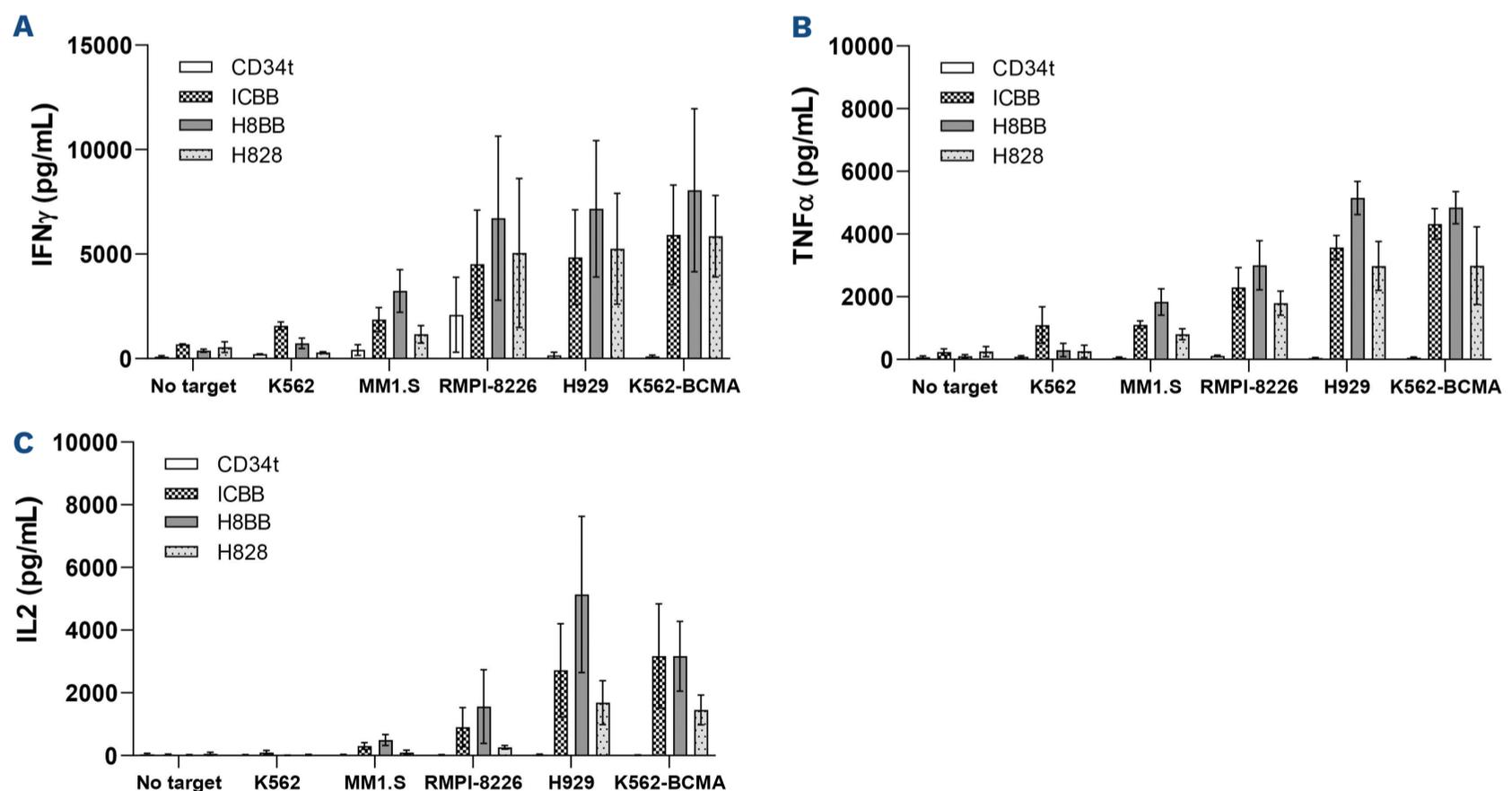

Figure 2. Anti-tumor function of BCMA-CAR-T cells. (A) OKT3-activated human primary B-cell maturation antigen (PBMC) were transduced with a retroviral vector encoding either ICBB-, H828-, H8BB-CAR, or truncated CD34 (CD34t control). Transduced T cells were co-cultured with different tumor lines as indicated. Interferon γ (IFNγ) secreted in the co-culture supernatant was measured by enzyme-linked immunosorbant assay (ELISA). These results are presented as mean+ standard error of the mean (SEM) (n=4, with 3 different donors). The difference between H8BB and H828 was found statistically significant (*P*=0.00098; calculated using a paired Student's *t*-test). (B and C) Similarly, these cells were co-cultured with the indicated target T cells and TNFα (B) and IL-2 (C) concentrations secreted in the culture supernatant were determined by ELISA. These results are presented as mean+SEM (n=3, with 3 different donors). *P*=0.01 for IL-2 and P=3.7x10^{-5} for TNFα; by paired Student's *t*-test). BCMA: B-cell maturation antigen; CAR: chimeric antigen receptor.

RPMI8226, we observed an average secretion of 6,721 pg/mL of IFNγ-mediated by the H8BB, 4,520 pg/mL by ICBB and 5,055 pg/mL by H828. Similar results were observed when measuring TNFα and IL-2 secretion and the difference between H8BB and H828 was found statistically significant (for IFNγ, $P=0.00098$; for IL-2, $P=0.01$ and for TNFα, $P=3.7x10^{-5}$; using a paired Student's t-test). As previously described herein (Figure 1B), it is noteworthy that H8BB- and H828- CAR-T cells displayed the lowest non-specific cytokine secretion in control co-cultures with an antigen-negative target (K562) or without any target (Figure 2A to C). This observation reinforces the idea that "off-target" (i.e., unspecific target) and tonic (i.e., without antigen stimulation) signaling may be influenced by the CAR configuration.

Phenotypic analysis of BCMA-engineered CAR-T cells
We then sought to characterize the phenotype of BCMA-CAR-T cells, focusing on CD4/CD8 ratio and on memory differentiation patterns. To this end, BCMA-CAR transduced T cells were sampled 3 weeks following PBMC activation and analyzed for marker expression by flow cytometry. As seen in Figure 3A, we did not notice any substantial differences between the different CAR-expressing populations as to the CD4/CD8 ratio which was approximately 1:2. Moreover, when analyzing the expression of the memory markers CD45RO

and CCR7, we observed a proportion of 44/40% of central memory (CM - CD45RO⁺/CCR7⁺) and 33/39% of effector memory (EM - CD45RO⁺/CCR7⁻) T cells in the ICBB- and H8BB-CART cells, respectively (Figure 3B). However, H828-transduced T cells displayed a higher proportion of effector memory T cells compared to 4-1BB-based CAR (57% *vs.* 36%; $P=0.037$) (Figure 3B). It has been reported that CAR-T cells displaying a "less differentiated profile" (namely, central memory cells), persist and, thus, perform better *in vivo*.[33] Exhausted T cells may become progressively dysfunctional, and this loss of function is mediated by the up-regulation of inhibitory receptors such as programmed death receptor-1 (PD-1), lymphocyte activation gene-3 (LAG-3), T-cell immunoglobulin-3 (TIM-3), and T-cell immunoreceptor with Ig and ITIM domains (TIGIT).[34] We therefore monitored the expression of these exhaustion markers over time in culture. Figure 3C shows a marked increase in the expression level of PD-1, LAG-3, TIM-3 and TIGIT on the surface of H828-transduced cell when compared to 4-1BB-based CAR over time ($P<0.001$). Importantly, H828-transduced T cells exhibited significantly higher levels of exhaustion markers at very early stages. This elevation in the basal expression of exhaustion markers may be mediated by tonic signaling augmented by the CD28 co-stimulatory portion of the CAR,[35] and notably, may impede with CAR-T-cell function *in vivo*.
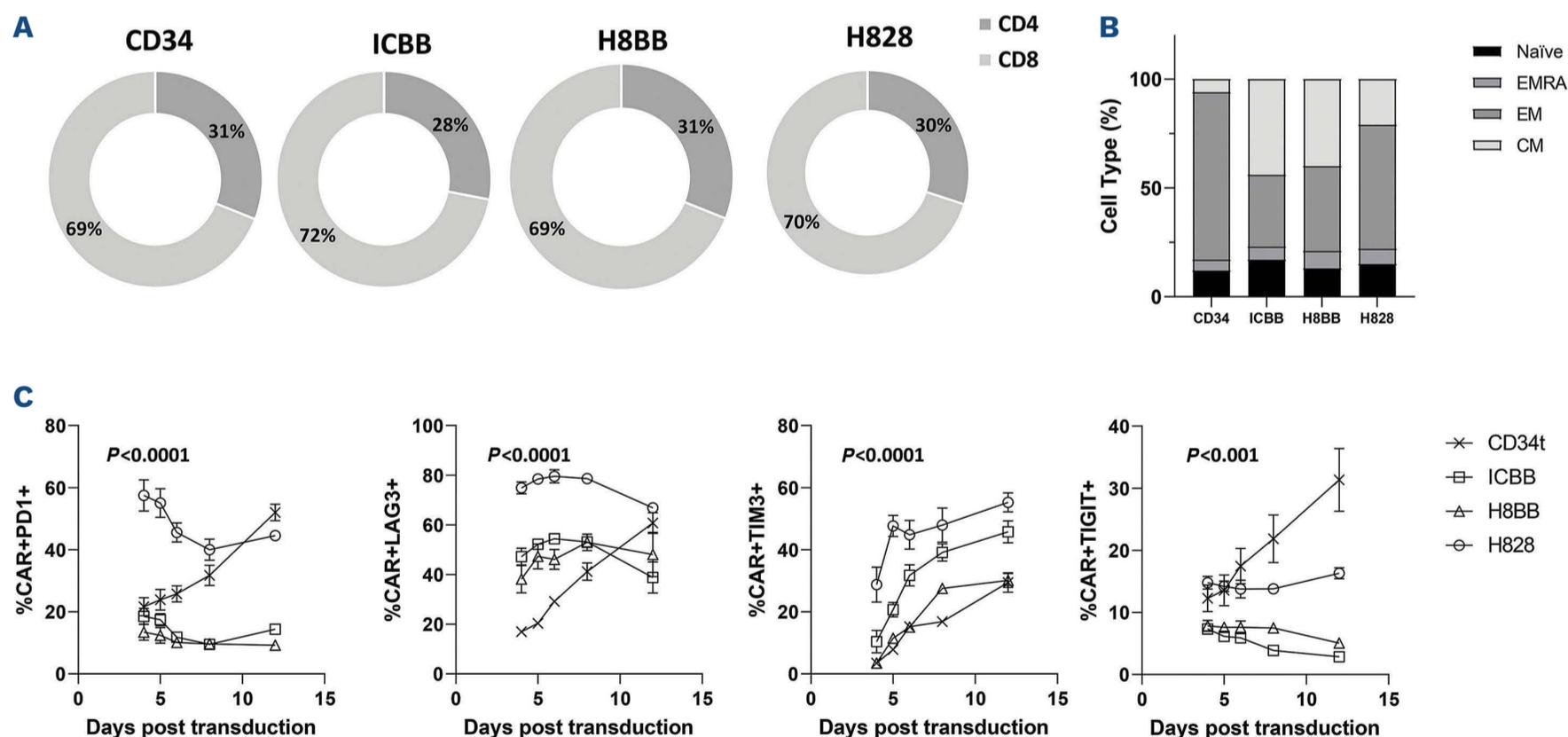

Figure 3. Phenotypic characterization of BCMA-CAR transduced T cells. (A) CD4/CD8 ratio of different anti-BCMA chimeras. CAR-transduced T cells or control T cells were stained with anti-CD4 and CD8 antibodies and analyzed by flow cytometry on day 7. These results are representative of 4 independent experiments with different donors. No significant difference was observed between the different groups. (B) Memory phenotype of T cells transduced with different BCMA chimeras. Three weeks following transduction, CAR-transduced T cells or control T cells were stained with anti-CD45RO and CCR7 antibodies and analyzed by flow cytometry. These results are representative of the mean of 4 independent experiments with different donors (n=4). (C) BCMA-CAR T cells in culture were monitored for the expression of exhaustion markers PD-1, LAG-3, TIM-3 and TIGIT over time (as indicated). BCMA: B-cell maturation antigen; CAR: chimeric antigen receptor.

Upregulation of activation markers and exhaustion profile of anti-BCMA chimeras following antigen stimulation

In order to further investigate how the basal expression of exhaustion markers may be correlated with their functionality, we analyze the expression of PD-1, LAG-3, TIM-3 and TIGIT following an overnight co-culture with BCMA-positive targets. Figure 4A indicates that all the four exhaustion markers are highly expressed on the surface of H828-CAR-T cells, even in the absence of target, as previously hinted in Figure 3C. However, 4-1BB-based CAR-T cells responded specifically to the different stimulations, by upregulating PD-1, LAG-3 and TIM-3 in a BCMA-dependent manner as expected. Interestingly, we also noted the basal expression of TIM-3 in ICBB-CAR-T cells was significantly higher than in H8BB-CAR-T cells (*P*<0.05). Given the fact that TIM-3 expression can also be induced upon activation,[36] this observation may account for the non-specific activity observed in cytokine release (Figure 1C; Figure 2A and B).

In order to test the hypothesis that basal expression of exhaustion markers may modulate CAR-T-cell activation state (Figure 3C), we next examined to what extent these CAR could mediate the upregulation of T-cell activation markers upon antigen stimulation. Following an overnight or a 4-hour co-culture with BCMA-positive target cells, BCMA-CAR-T cells were analyzed for surface expression of activation markers including CD25, CD69 and 4-1BB (i.e., CD137). As anticipated, we found a correlation between the activation status and the exhaustion profile of CAR-T cells. Indeed, Figure 4B (right panel) indicates that although H828-CAR-T cells can upregulate 4-1BB following stimulation with BCMA-expressing targets, they did so to a lesser extent than 4-1BB-based CAR-T cells (H828 *vs.* ICBB and H8BB, *P*<0.05). Similar results were achieved when measuring CD69 expression following short co-cultures (4 hours) of myeloma target cells (Figure 4B, middle panel). Additionally, we noted that H8BB-CAR-T cells could significantly upregulate CD25 (*P*<0.01), while ICBB- and H828-CAR-T
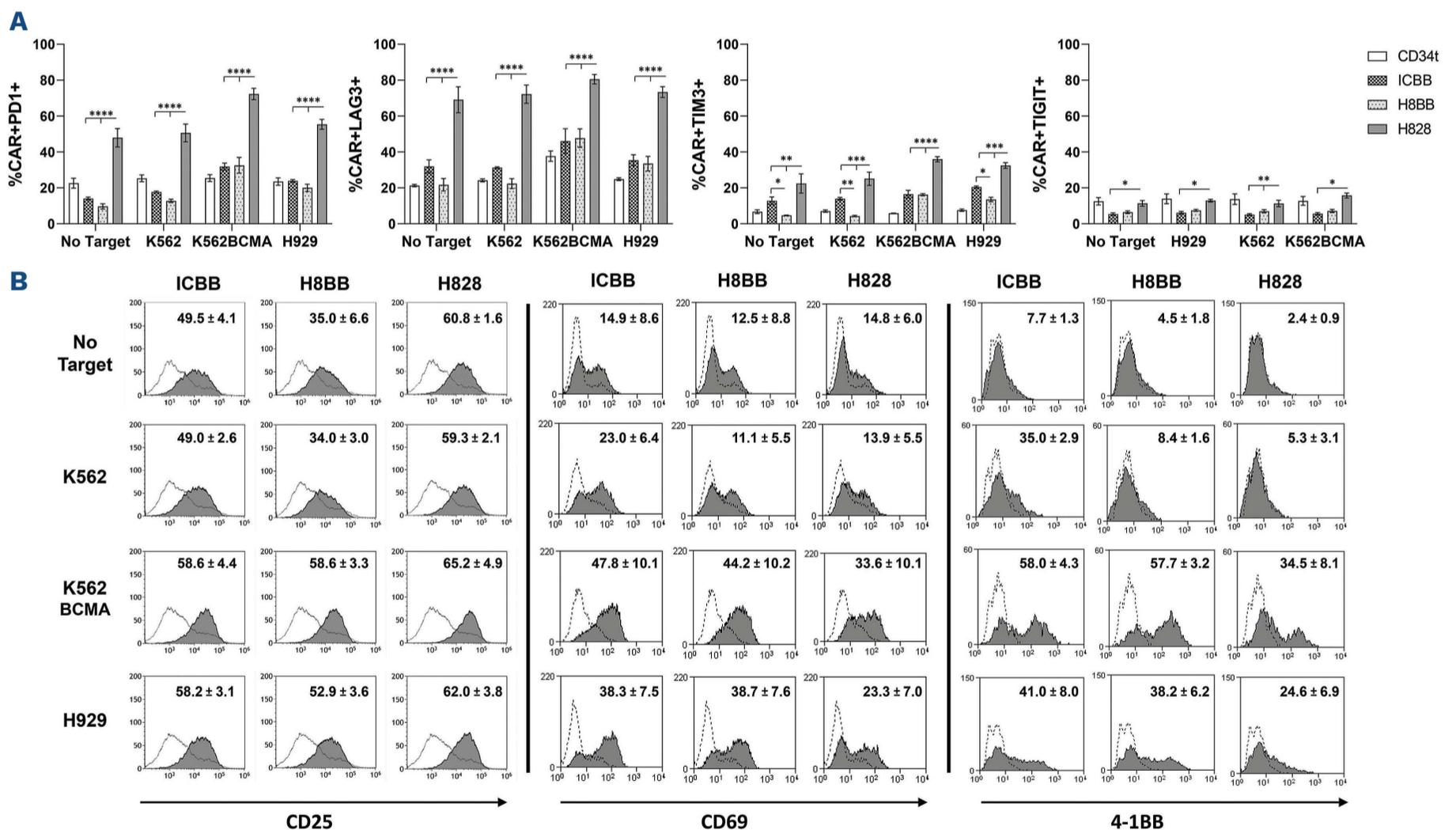

Figure 4. Exhaustion and activation profile of BCMA-CAR-T cells. (A) BCMA-CAR-T cells were co-cultured for 24 hours in the presence of the H929-MM cell line or BCMA-overexpressing K562 (K562-BCMA), or K562 cell line in T-cell medium without IL-2 at an effector to target (E:T) ratio of 10:1, in T-cell medium without IL-2, at 37°C. Following incubation, cells were washed, stained at 4°C for 20 minutes with a mixture of the fusion protein/antibodies (as indicated), to assess the expression of PD-1, LAG-3, TIM-3 and TIGIT by flow cytometry (gated on BCMA.CAR+). These results are representative of 3 different experiments with different donors. Data is represented as mean values ± standard error of the mean (SEM). (B) CAR-transduced T cells or CD34t cells were co-cultured with BCMA-positive targets, as indicated. Following an overnight or 4-hour co-culture (for CD69), cells were analyzed by flow cytometry for the expression of 4-1BB (right panel), CD69 (middle panel) and CD25 (left panel). Cells were gated on the CD8+ population for 4-1BB and CD69 expression, and on CAR+ cells for CD25 expression. The mean percentage of positive cells ± SEM is indicated on histograms overlay. Grey filled histograms represent CAR-T cells staining, and the dotted line histograms represent the staining of the CD34t control cells. These results are representative of 3 independent experiments with 3 different donors. BCMA: B-cell maturation antigen; CAR: chimeric antigen receptor.

cells did not respond significantly to antigen stimulation (Figure 4B, left panel). For example, whereas CD25 expression levels were generally higher following co-culture with BCMA-positive targets in H828-CAR-T cells (between 62-65%) in comparison with H8BB-CAR-T cells (52.9-58.6% - H828 *vs.* H8BB, *P*<0.001), they did not increase significantly from those observed for unstimulated cells or in co-culture with BCMA-negative cells (59.3-60.8%). Thus, these results indicate that H8BB exhibited the lowest levels of exhaustion receptors and increased upregulation of activation markers which may facilitate a better specific and long-term *in vivo* activity.

H8BB-CAR mediates improved *in vitro* cytotoxicity and *in vivo* biological activity

In order to assess our assumption that H8BB would display an efficient and safe profile at mediating tumor eradication, we examined the cytotoxic activity of the T cells

transduced with the different BCMA-CAR. Thus, tumor target cells, labeled with CFSE, were co-cultured with BCMA CAR- or CD34t control T cells for 4 hours. Then, CFSE-positive cells were analyzed for PI staining, as a surrogate for cytotoxic activity. As observed in Figure 5A, all CAR constructs mediated significant cytotoxicity against the H929 and RPMI-8226 myeloma cell lines, in comparison with CD34t control T cells (*P*<0.0001). Moreover, 4-1BB-based CAR-T cells demonstrated significantly higher cytotoxicity against RPMI-8226 myeloma cells even at the lowest ratio 2.5:1 (ICBB or H8BB *vs.* CD34t, *P*<0.001). Similar results were obtained when H8BB-CAR T cells were co-cultured with H929 (Figure 5A, bottom panel; H8BB *vs.* CD34t, *P*<0.05). Additionally, H8BB, but not ICBB, was more efficient than H828 at mediating cytotoxicity against RPMI-8226 at escalating E:T ratios (Figure 5A, middle panel; H8BB *vs.* H828 both at 5:1 and 10:1 ratio, *P*<0.05). As expected, CAR-T cells did not show any significant
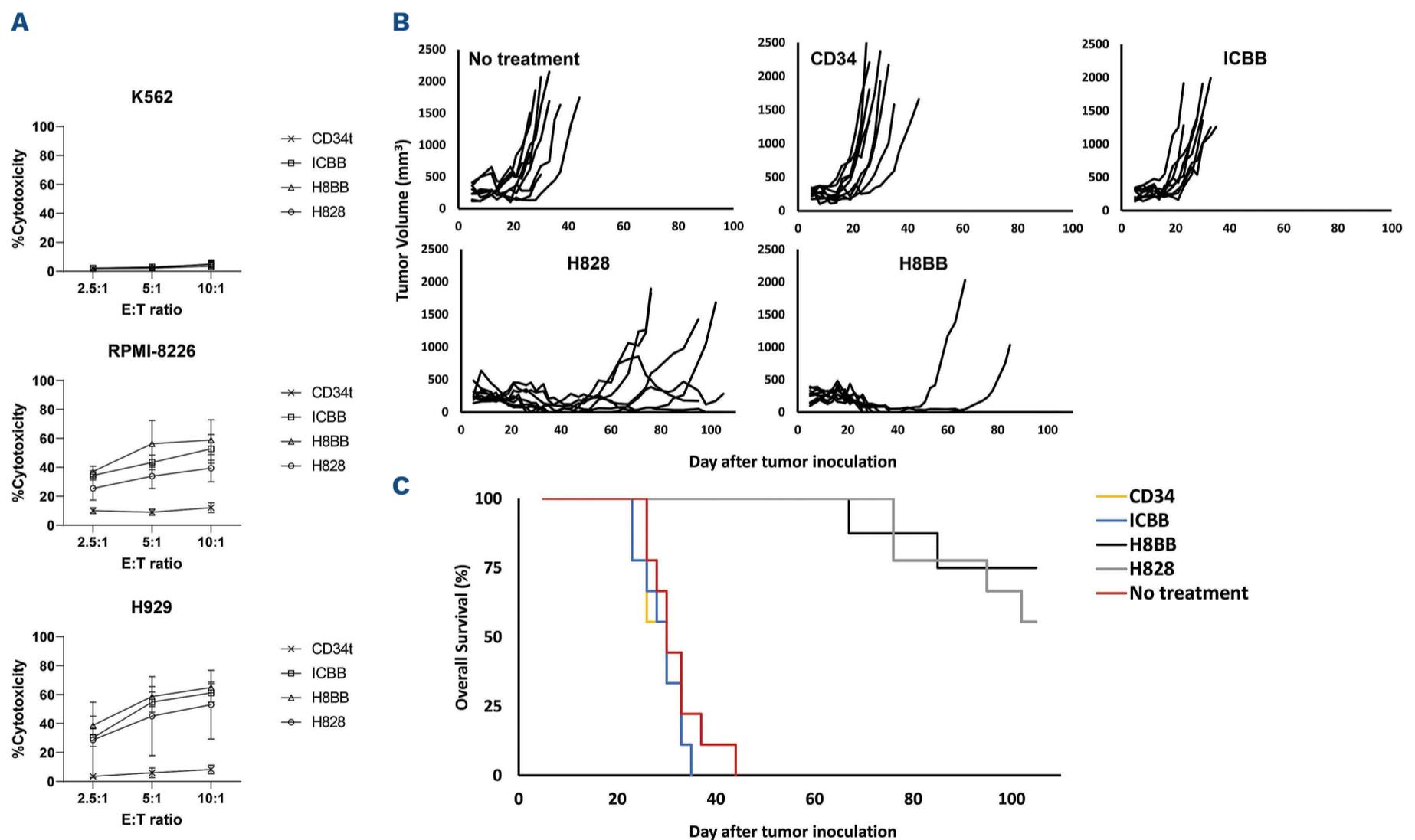

Figure 5. BCMA chimeras mediate anti-tumor cytotoxic activity *in vitro* and *in vivo*. (A) BCMA CAR or CD34t (control) transduced T cells were co-cultured with CFSE-labeled tumor cells at the indicated effector to target (E:T) ratios. After 4 hours, propidium iodide (PI) was added and the cells were analyzed by flow cytometry. Cytotoxicity was calculated based on the proportion of CFSE[+]/PI[+] population out of the total CFSE[+] population. These results are presented as mean ± standard error of the mean (SEM) of 3 independent experiments with 3 different donors and the difference between the BCMA-CARs and CD34t populations was found statistically significant (*P*<0.05, calculated using a Student's paired *t*-test). (B) *In vivo* function of BCMA-CAR-T cells. NSG xenografts (n=8-9 per group) were inoculated H929 myeloma cells. One week following tumor inoculation, the mice were intravenously injected either with 15×10^6 BCMA-CAR+ or with CD34t-transduced control cells. Tumor volume was measured in a blinded fashion using a caliper and calculated using the following formula: $(D\times d^2)\times\Pi/6$, where D is the largest tumor diameter and d its perpendicular one. (C) Overall survival analysis. The difference in the average survival of the H828 and H8BB groups compared to the no-treatment or control groups was found statistically significant (*P*<1e[-4], using a logrank analysis). BCMA: B-cell maturation antigen; CAR: chimeric antigen.

cytotoxicity against the BCMA-negative cell line K562 (Figure 5A, top panel) when compared to corresponding control T cells. These results suggest that H8BB displays an advantage over H828 and ICBB at mediating myeloma cells elimination *in vitro*, even at low E:T ratio. Since cytotoxicity is mediated via the spatial recognition between the CAR molecule on the effector cells and cognate antigen at the surface of the target cells, we concluded that the configuration of H8BB is adequate to allow BCMA recognition and induce myeloma killing.

Finally, we analyzed BCMA-CAR function *in vivo*, using a xenograft model of human tumors. Immunodeficient NSG mice were inoculated with 4×10^6 NCI-H929 cells. Five days later, these mice were adoptively transferred intravenously either with BCMA-CAR or control T cells (CD34t-transduced T cells) or were left untreated ("no treatment"). Tumor volume was blindly evaluated every 2-3 days. H8BB- or H828-CAR-T cells display a significant delay and/or a marked regression in the tumor volume

(H8BB *vs.* control groups, $P<0.0001$ and H828 *vs.* control groups, $P<0.001$; Figure 5B), when compared to the control groups ("no treatment" and or CD34t groups) or the ICBB group. This observation is also reflected by the improved overall survival (Figure 5C; H8BB and H828 groups *vs.* control groups, $P<0.0001$; by log-rank analysis). Puzzlingly, ICBB CAR-T cells showed no significant anti-tumor activity compared to the control group. Furthermore, we found a significant reduction in the tumor volume of H8BB-treated mice in comparison with the tumor volume of H828-treated cohort (H8BB *vs.* H828, $P<0.05$; by Kruskal-Wallis test, with Dunn's *post hoc* analysis). In this regard, we observed that out of the nine mice that were administered either with H8BB or H828 CAR-T cells, four mice in the H828 group relapsed, and two additional mice showed fluctuations in their tumor volumes, while only two mice in the H8BB group experienced relapses (Figure 5B). Thus, we conclude that, while ICBB could not mediate myeloma eradication *in vivo*, H8BB was proven significantly more
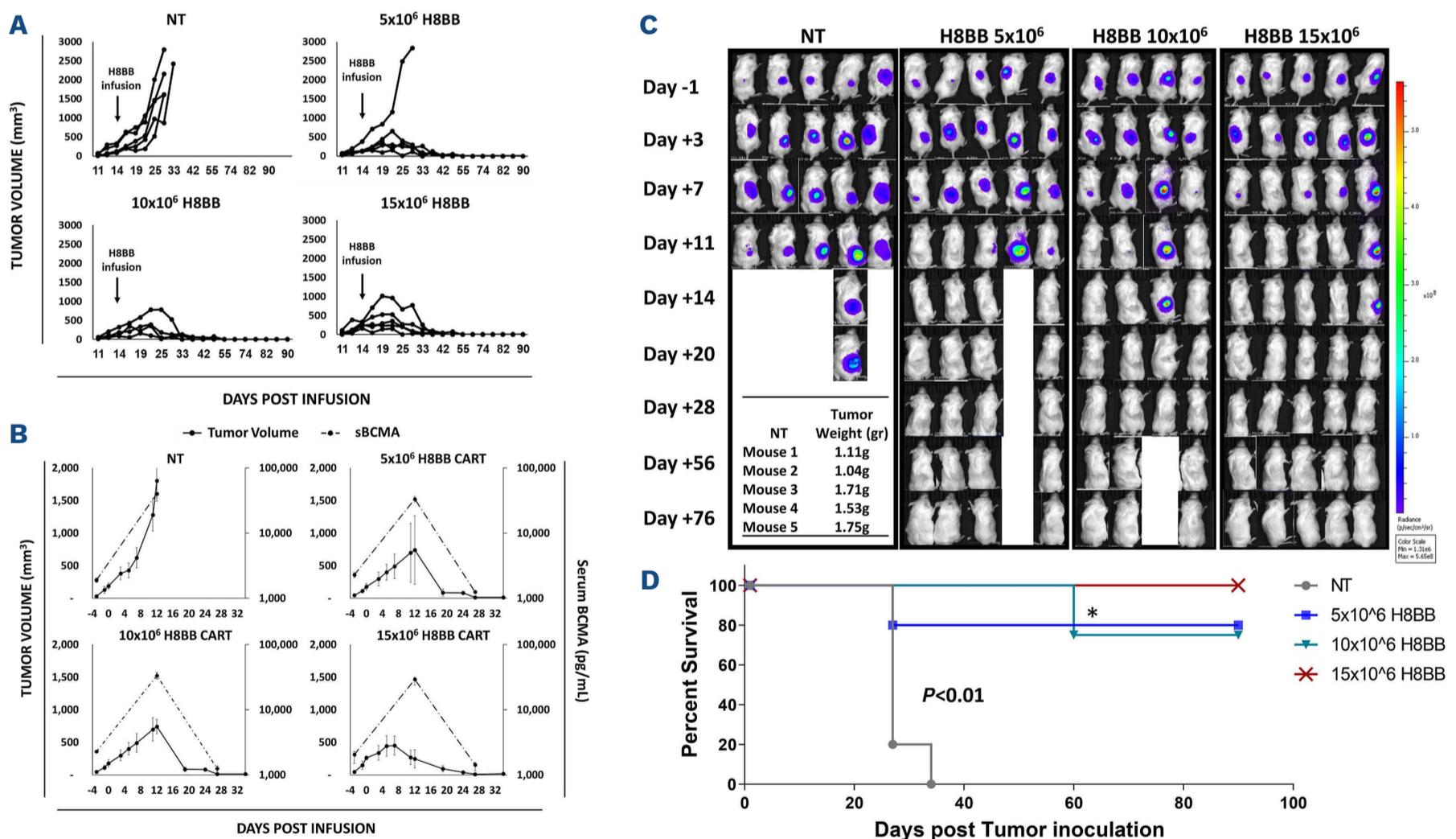

Figure 6. Anti-myeloma effect of H8BB CAR-T cells. (A) NSG mice (4-5 animals per group) with an average of approximately 200 mm³ subcutaneous NCI-H929 tumors per treatment group received a single intravenous (*i.v.*) administration of 15×10^6 non-transduced (NT) control cells, or 5, 10 or 15×10^6 H8BB-CAR⁺ T cells/mouse, respectively. Tumor size was measured by calipers twice weekly by personnel blinded to treatment conditions. (B) Serum B-cell maturation antigen (BCMA) protein levels assessed by enzyme-linked immunosorbant assay (grey dashed line) were plotted with corresponding tumor volume measurements (black line). Error bars show standard error of the mean (SEM). (C) Myeloma development was monitored by bioluminescence imaging (BLI). BLI measurement in photons per second per cm² per steradian (p/s/cm²/sr) was translated to color to indicate disease activity in the mice by the legend shown. The weight of the tumors that were excised from NSG xenografts in the NT group is indicated in the table, to show that BLI reduction at this time was rather due to tumor necrosis than to a reduction in the tumor size. (D) Kaplan–Meier survival curves of study shown in (A and C); * represents NSG mouse that was found dead at day 60 post tumor inoculation, without any apparent relation to multiple myeloma.

efficient than H828 in mediating significant *in vivo* anti-tumor activity.

Further evaluation of the anti-tumor/off-target activity of H8BB CAR-T cells *in vivo*

Given the optimal profile of H8BB compared to the other BCMA CAR assessed herein (i.e., appropriate optimal cell growth [Figure 1C], antitumor cytokines production with a minimal non-specific secretion [Figure 2A to C], reduced exhaustion profile [Figure 4A], reduced tonic signaling and non-specific activation [Figure 4B], high antitumoral cyto-toxic activity both *in vitro* and *in vivo* [Figure 5A to C]), we decided to focus our efforts at evaluating H8BB potential therapeutic value to target BCMA in the treatment of plasma cell malignancies. In this attempt, we opted to study the anti-tumor function mediated by H8BB CAR-T cells and aimed at determining the optimal effective dose of H8BB CAR-T cells for infusion to achieve a desired therapeutic effect. To that end, we established an additional model in which NSG mice were injected with 4×10^6 luciferase-expressing NCI-H929 myeloma cells. We chal-

lenged H8BB CAR-T cells by subjecting them to a higher tumor load than detailed above in Figure 5B and C. Only once the tumors were well-established (164 ± 30 mm^3, about 2 weeks following inoculation), the mice were infused with escalating doses of H8BB CAR-T cells (5, 10 or 15×10^6 cells) or non-transduced (NT) cells as control. As shown in Figure 6, H8BB CAR-T cells exhibited a strong anti-myeloma effect. Specifically, the mice groups that received a single injection of 10×10^6 or 15×10^6 H8BB CAR-T cells, showed an initial increase in tumor volume followed by a rapid and complete tumor regression by 2 to 3 weeks post infusion (Figures 6A to C). In the mice group that received 5×10^6 CAR-T cells, four of five mice showed complete tumor regression. These results indicate that the minimal effective dose against NCI-H929 ranges between $5-10 \times 10^6$ cells. As for the control group, the mice were all sacrificed within a month post tumor inoculation for ethical reasons. In parallel, we evaluated the concentration of soluble BCMA (sBCMA) in the serum as a biomarker for MM[37] and evidence for tumor eradication. sBCMA levels rapidly declined in concomitance with tumor regression
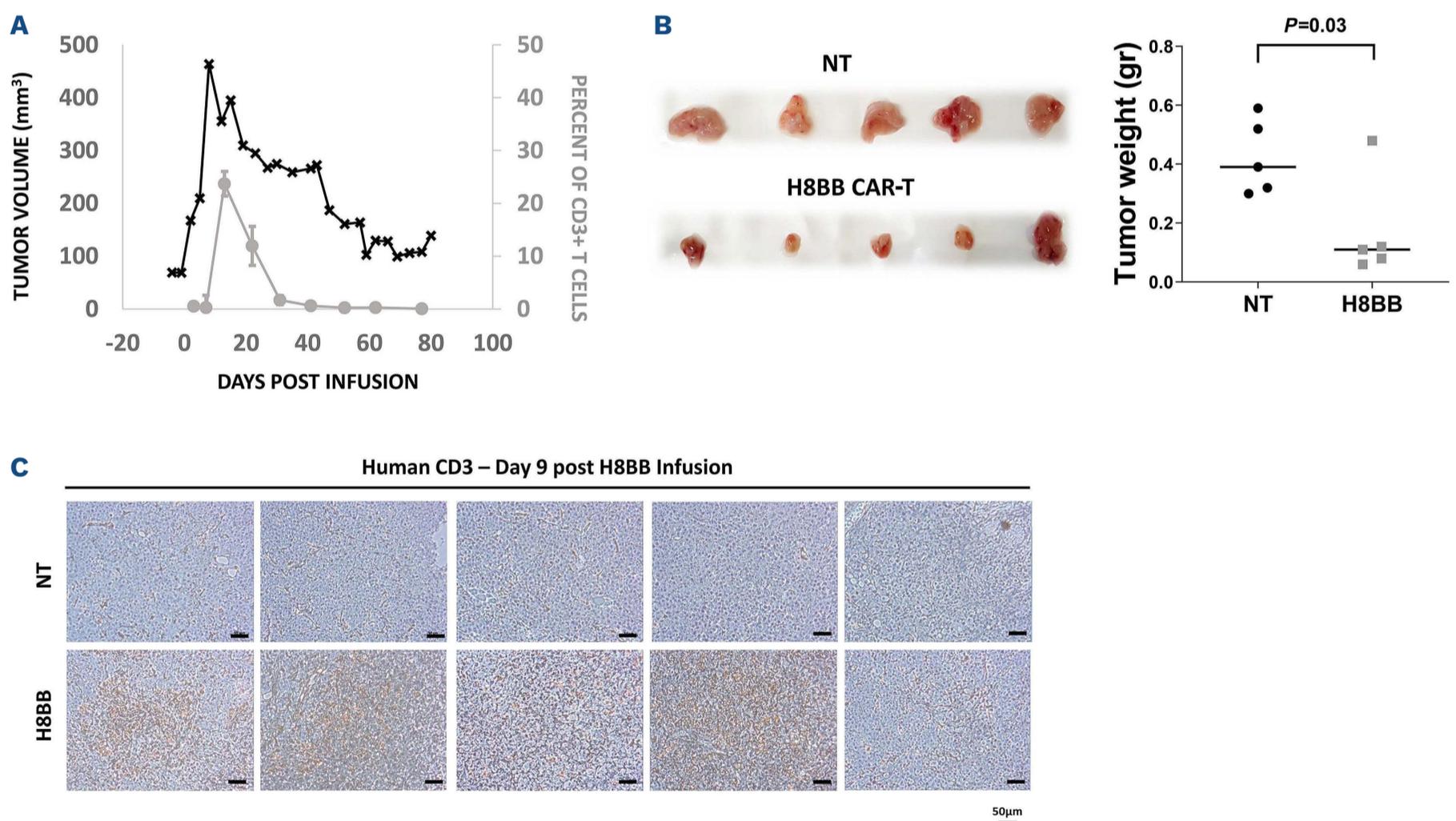
Figure 7. CAR$^+$-T cells persistence in mice is associated with the elimination of NCI-H929 multiple myeloma tumor. (A) 25 µL of blood were collected from the tail vein was lysed with IOTEST 3 Lysing Solution (Beckman Coulter) for 10 minutes and stained with a mixture of fluorescent recombinant human B-cell maturation antigen (BCMA) protein, anti-CD3, anti-CD8 and anti-CD4. The percent of H8BB CAR-T cells in NSG blood (% of CD3$^+$BCMA.CAR$^+$ cells) was assessed by flow cytometry. (B) Average weight of the tumors excised from NCI-H929 multiple myeloma (MM) xenografts at day 9 post T-cell infusion. H8BB CAR-T xenograft tumors are shown in the bottom panel; non-transduced (NT) xenograft control tumors are shown in the upper panel. (C) Infiltration of tumor tissue (depicted in B, upper panel) by CD3$^+$ T cells was assessed by immunohistochemistry using anti-human CD3 antibody by day 9 post H8BB CAR or NT T-cell infusion. Marker bar represents 50 µm. Note: Figure 7A to C refer to experiments performed on different cohorts of mice.

following CAR-T cell infusion (Figure 6B). Also, this data confirms that high concentrations of sBCMA in the blood of NSG xenografts did not seem to block the anti-myeloma activity of H8BB CAR-T cells *in vivo*.

We investigated the persistence of H8BB CAR-T cells in mice xenografts both intratumorally and in the blood. CAR-T cells were detected in the periphery 3 days after T-cell injection, significantly increased 13-22 days after adoptive transfer and then declined over the next 3 weeks (Figure 7A). In a parallel cohort of NSG MM xenografts, mice were treated with 7.5×10^6 H8BB-CAR-T cell or control and sacrificed at day 9 following T-cell administration. Figure 7B indicates that the average weight of tumors (following excision) from H8BB-CAR T-treated mice was significantly lower than in the control group (*P*=0.03). Immunohistochemistry performed on tumor sections shows that human T cells were abundantly present in the H8BB sections (Figure 7C, bottom panel) while sparse in the control group (Figure 7C, upper panel). Altogether, these data demonstrate that H8BB CAR-T actively proliferate, traffic to tumor sites and mediate tumor eradication.

Anti-myeloma efficacy of H8BB CAR-T cell against primary cells from multiple myeloma patients

As a preclinical evaluation step for the possible implementation of H8BB CAR-T cells treatment for myeloma patients, BCMA expression was assessed on plasma cells from the BM of patients suffering from different pathologies (e.g., MM, amyloidosis [AL], monoclonal gammopathy of undetermined significance [MGUS], plasmacytoma [PC] and Waldenström's macroglobulinemia [WDS]). In line with previous data,[38] we observed a differential median expression of BCMA on plasma cells (gated on $CD38^{++}CD138^{++}$) derived from the BM of MM, AL, MGUS, PC and WDS patients, with a mean fluorescence intensity
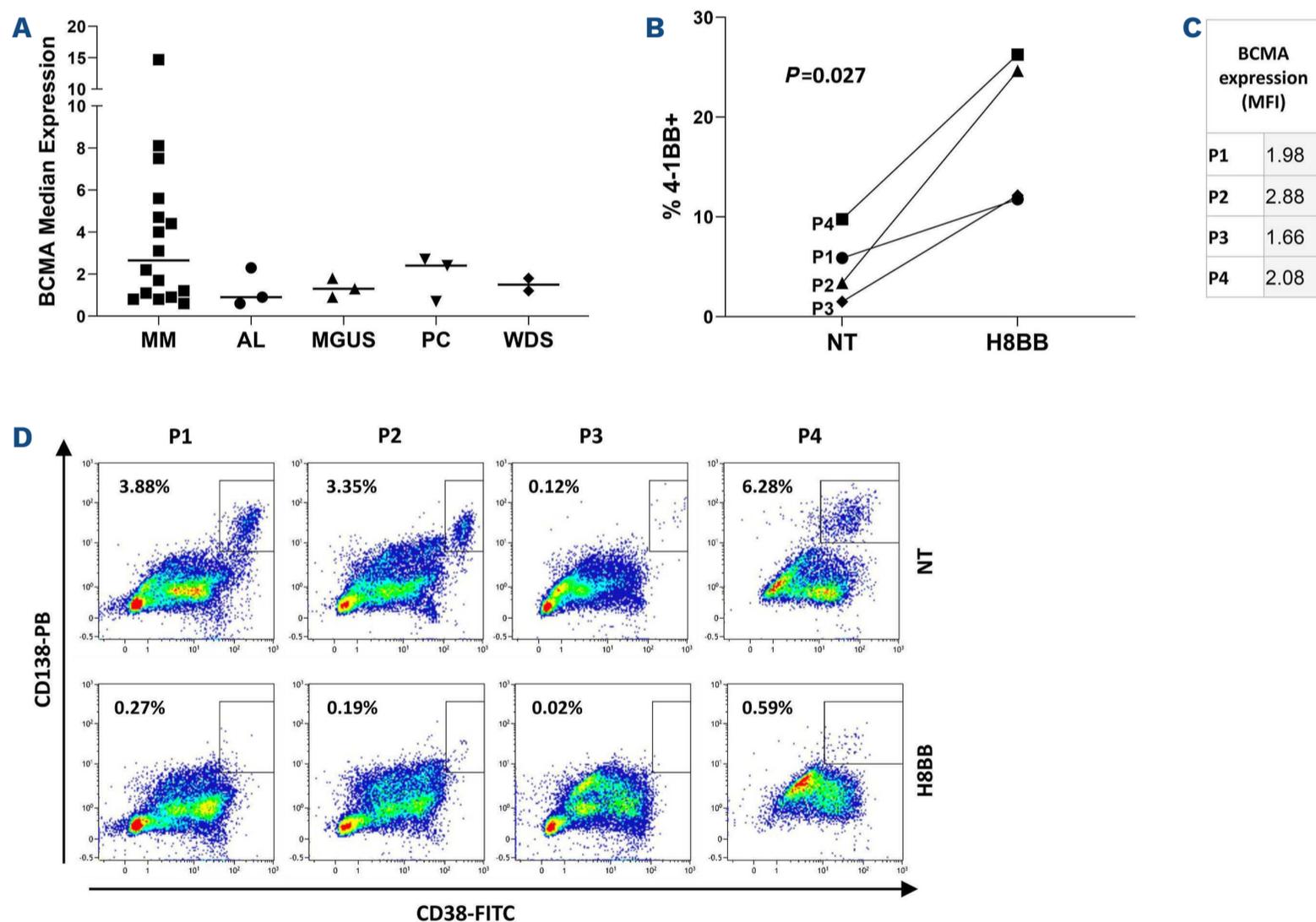
Figure 8. H8BB CAR-T cells target plasma cells of multiple myeloma patients. (A) Bone marrow (BM) aspirates of multiple myeloma (MM), amyloidosis (AL), monoclonal gammopathy of undetermined significance (MGUS), plasmacytoma (PC) and Waldenström's macroglobulinemia (WDS) patients were assessed for B-cell maturation antigen (BCMA) expression by flow cytometry. The graph represents BCMA median expression in the bone marrow of patients, gated on $CD38^{++}CD138^{++}$ plasma cells. n=3 (AL, circles), n=16 (MM, squares), n=3 (MGUS, up triangles), n=3 (PC, down triangles), and n=2 (WDS, lozenges). Error bars show standard error of the mean (SEM). (B) Activation of CD3+ T cells was determined by assessing the expression of CD137 (4-1BB) by flow cytometry. H8BB CAR-T and non-transduced (NT) T cells were incubated in the presence of BM-derived mononuclear cells (BM-MC) overnight. Statistical analysis was based on a Student's paired *t*-test. (C) Mean fluorescence intensity (MFI) of BCMA expression on the targeted $CD38^{++}CD138^{++}$ plasma cell population of patients P1 to P4 (*P*=0.01, by Student's *t*-test). (D) The presence of $CD38^{++}CD138^{++}$ plasma cells of MM patients following co-culture with H8BB CAR-T cells or NT control cells was assessed by flow cytometry (P1 to P4).

(MFI) of 3.8±3.8, 1.2±0.9, 1.3±0.4, 1.9±1.1 and 1.5±0.4 respectively (Figure 8A). Although the average of BCMA-MFI in MM patients is markedly higher in comparison with other plasma cell disorders, *P*-values do not meet significance. We investigated whether H8BB-CAR-T cells could efficiently target primary myeloma cell: BM-MNC from MM patients were co-cultured with either H8BB CAR-T cells or NT (control) in an allogeneic system (Figure 8B to D). Figure 8B indicates that H8BB T cells could significantly upregulate 4-1BB expression compared to NT (control) cells, when co-cultured with BM-MNC of MM patients (*P*=0.027). Figure 8C shows the level of BCMA expression on patients' BM-MNC (gated on CD38$^+$CD138$^+$). Overnight co-incubation of BM-MNC with H8BB CAR-T cells resulted in almost complete elimination of the plasma cells (gated on CD38^{++}/CD138^{++}; Figure 8D, right panel). In contrast, plasma cells were not affected by the presence of NT cells (Figure 8D, left panel), demonstrating the specificity of BCMA-CAR targeting. Altogether, these data confirm the potential efficacy of H8BB CAR-T-based therapy for the treatment of multiple myeloma.

Discussion

CAR-T-cell strategies revolutionized the treatment of CD19$^+$ lymphoma and leukemia. The application of such approaches to other hematological malignancies such as MM requires the identification and design of suitable CAR targeting specific antigens. Herein, we designed and evaluated the theraputic function of several BCMA-specific CAR based on the same antibody chains forming the targeting moiety. Two of the assessed CAR incorporated a CD28 moiety (IC28 and H828) while the other two (ICBB and H8BB) were 4-1BB-based. Initial testing indicated the IC28 was the least functional (Figure 1B), prompting us to focus on the other constructs.

Compared to the evaluated CAR herein, H8BB demonstrated generally the highest biological activity by means of cytokine secretion, cytotoxicity, and upregulation of activation markers. Puzzlingly, while both the H8BB and H828 constructs mediated tumor regression in xenograft experiments, ICBB did not display significant *in vivo* activity (Figure 5). Several reasons could account for that: indeed, both H8BB and H828 share hinge and transmembrane regions derived from CD8 while the ICBB uses a shorter hinge (21 aa *vs.* 46 aa) and a CD28 TM region. Several studies demonstrated the need to custom-tailor the hinge nature and length to the targeted antigen.[39,40] It was also shown that a longer hinge may increase CAR potency and specificity[41] and that CD8 hinge can lead to less activation-induced cell death.[19] It was recently demonstrated that modifications in CD8α hinge and TM domains result in higher anti-apoptotic molecule

expression in CAR-T cells and reduced cytokine secretion, along with retained cytotoxic function.[42] ICBB poor *in vivo* performance might also be related to less expansion potential (Figure 1D and E), tonic signaling and non-specific activity (Figure 2A and B), which could eventually lead to hypofunction.[35]

When comparing H8BB and H828, we noted the former generally demonstrated superior activity with significantly lower exhaustion marker levels. Both demonstrated *in vivo* activity, with H8BB-CAR leading to better survival and a more pronounced effect on tumor regression. Thus, this seems to corroborate the previously described long term advantage manifested 4-1BB-based CAR over CD28-based receptors.[17]

We further explored the therapeutic potential of H8BB in preclinical studies. Importantly, we confirmed that BCMA can be expressed by plasma cells from the bone marrow of patients suffering from different plasma cells pathologies (Figure 8A). Considering the encouraging data collected so far as to the functionality, specificity, and efficacy of H8BB, we aim to assess the therapeutic potential of an H8BB CAR-T cell-based treatment in patients with different plasma cell pathologies including not only MM, but also other disorders such as light-chain amyloidosis. To this end and following the approval from the Israeli Ministry of Health, we initiated a clinical study, enrolling R/R malignant plasma cell patients to be treated with autologous H8BB CAR-T cells (clinicaltrails gov. Identifier: NCT04720313) in a dose escalation study first evaluating the safety, and then the efficacy of this approach. In conclusion, based on the results presented herein, we are confident that CAR-T therapy based on the optimized receptor H8BB holds promise for the treatment of MM and additional plasma cell-related pathologies.

Data-sharing statement

For original data, please contact the corresponding authors.

References

1. Bu DX, Singh R, Choi EE, et al. Pre-clinical validation of B cell maturation antigen (BCMA) as a target for T cell immunotherapy of multiple myeloma. Oncotarget. 2018;9(40):25764-25780.
2. Palumbo A, Anderson K. Multiple myeloma. N Engl J Med. 2011;364(119):1046-1060.
3. Cho SF, Anderson KC, Tai YT. Targeting B cell maturation antigen (BCMA) in multiple myeloma: potential uses of BCMA-based immunotherapy. Front Immunol. 2018;9:1821.
4. Meinl E, Thaler FS, Lichtenthaler SF. Shedding of BAFF/APRIL receptors controls B cells. Trends Immunol. 2018;39(9):673-676.
5. Friedman KM, Garrett TE, Evans JW, et al. Effective targeting of multiple B-cell maturation antigen-expressing hematological malignances by anti-B-cell maturation antigen chimeric antigen receptor T cells. Hum Gene Ther. 2018;29(5):585-601.
6. Ghosh A, Mailankody S, Giralt SA, et al. CAR T cell therapy for multiple myeloma: where are we now and where are we headed? Leuk Lymphoma. 2018;59(9):2056-2067.
7. Carpenter RO, Evbuomwan MO, Pittaluga S, et al. B-cell maturation antigen is a promising target for adoptive T-cell therapy of multiple myeloma. Clin.Cancer Res. 2013;19(8):2048-2060.
8. Ali SA, Shi V, Maric I, et al. T cells expressing an anti-B-cell maturation antigen chimeric antigen receptor cause remissions of multiple myeloma. Blood. 2016;128(13):1688-1700.
9. Brudno JN, Maric I, Hartman SD, et al. T cells genetically modified to express an anti-B-cell maturation antigen chimeric antigen receptor cause remissions of poor-prognosis relapsed multiple myeloma. J Clin Oncol. 2018;36(22):2267-2280.
10. Raje N, Berdeja J, Lin Y, et al. Anti-BCMA CAR T-cell therapy bb2121 in relapsed or refractory multiple myeloma. N Engl J Med. 2019;380(18):1726-1737.
11. Cohen AD, Garfall AL, Stadtmauer EA, et al. B cell maturation antigen-specific CAR T cells are clinically active in multiple myeloma. J Clin Invest. 2019;129(6):2210-2221.
12. Jiang S, Jin J, Hao S, et al. Low dose of human scFv-derived BCMA-targeted CAR-T cells achieved fast response and high complete remission in patients with relapsed/refractory multiple myeloma. Blood. 2018;132(Suppl 1):S960.
13. Liu Y, Chen Z, Fang H, et al. Durable remission achieved from Bcma-directed CAR-T therapy against relapsed or refractory multiple myeloma. Blood. 2018;132(Suppl 1):S956.
14. Mailankody S, Ghosh A, Staehr M, et al. Clinical responses and pharmacokinetics of MCARH171, a human-derived Bcma targeted CAR T cell therapy in relapsed/refractory multiple myeloma: final results of a phase I clinical trial. Blood. 2018;132(Suppl 1):S959.
15. Munshi NC, Anderson LD, Jr., Shah N, et al. Idecabtagene vicleucel in relapsed and refractory multiple myeloma. N Engl J Med. 2021;384(8):705-716.
16. Berdeja JG, Madduri D, Usmani SZ, et al. Ciltacabtagene autoleucel, a B-cell maturation antigen-directed chimeric antigen receptor T-cell therapy in patients with relapsed or refractory multiple myeloma (CARTITUDE-1): a phase 1b/2 open-label study. Lancet. 2021;398(10297):314-324.
17. Kawalekar OU, O'Connor RS, Fraietta JA, et al. Distinct signaling of coreceptors regulates specific metabolism pathways and impacts memory development in CAR T cells. Immunity. 2016;44(2):380-390.
18. Fujiwara K, Tsunei A, Kusabuka H, et al. Hinge and transmembrane domains of chimeric antigen receptor regulate receptor expression and signaling threshold. Cells. 2020;9(5):1182.
19. Alabanza L, Pegues M, Geldres C, et al. Function of novel anti-CD19 chimeric antigen receptors with human variable regions is affected by hinge and transmembrane domains. Mol Ther. 2017;25(11):2452-2465.
20. Hudecek M, Sommermeyer D, Kosasih PL, et al. The nonsignaling extracellular spacer domain of chimeric antigen receptors is decisive for in vivo antitumor activity. Cancer Immunol Res. 2015;3(2):125-135.
21. Hudecek M, Lupo-Stanghellini MT, Kosasih PL, et al. Receptor affinity and extracellular domain modifications affect tumor recognition by ROR1-specific chimeric antigen receptor T cells. Clin Cancer Res. 2013;19(12):3153-3164.
22. James SE, Greenberg PD, Jensen MC, et al. Antigen sensitivity of CD22-specific chimeric TCR is modulated by target epitope distance from the cell membrane. J Immunol. 2008;180(10):7028-7038.
23. Davey AS, Call ME, Call MJ. The influence of chimeric antigen receptor structural domains on clinical outcomes and associated toxicities. Cancers (Basel) 2020;13(1):38.
24. Daniel-Meshulam I, Horovitz-Fried M, Cohen CJ. Enhanced antitumor activity mediated by human 4-1BB-engineered T cells. Int J Cancer. 2013;13(12):2903-2913.
25. Eisenberg V, Shamalov K, Meir S, et al. Targeting multiple tumors using T-cells engineered to express a natural cytotoxicity receptor 2-based chimeric receptor. Front Immunol. 2017;8:1212.
26. Meril S, Harush O, Reboh Y, et al. Targeting glycosylated antigens on cancer cells using siglec-7/9-based CAR T-cells. Mol Carcinog. 2020;59(7):713-723.
27. Liu L, Sommermeyer D, Cabanov A, et al. Inclusion of Strep-tag II in design of antigen receptors for T-cell immunotherapy. Nat Biotechnol. 2016;34(4):430-434.
28. Hoogi S, Eisenberg V, Mayer S, et al. A TIGIT-based chimeric co-stimulatory switch receptor improves T-cell anti-tumor function. J Immunother Cancer. 2019;7(1):243.
29. Shamalov K, Levy SN, Horovitz-Fried M, Cohen CJ. The mutational status of p53 can influence its recognition by human T-cells. Oncoimmunology. 2017;6(4):e1285990.
30. Tal Y, Yaakobi S, Horovitz-Fried M, et al. An NCR1-based chimeric receptor endows T-cells with multiple anti-tumor specificities. Oncotarget. 2014;5(21):10949-10958.

31. Eisenberg V, Hoogi S, Shamul A, Barliya T, Cohen CJ. T-cells "a la CAR-T(e)" - genetically engineering T-cell response against cancer. Adv Drug Deliv Rev. 2019;141:23-40.

32. Wilde S, Sommermeyer D, Leisegang M, et al. Human antitumor CD8+ T cells producing Th1 polycytokines show superior antigen sensitivity and tumor recognition. J Immunol. 2012;189(2):598-605.

33. Ren H, Cao K, Wang M. A correlation between differentiation phenotypes of infused T cells and anti-cancer immunotherapy. Front Immunol. 2021;12:745109.

34. Anderson AC, Joller N, Kuchroo VK. Lag-3, Tim-3, and TIGIT: co-inhibitory receptors with specialized functions in immune regulation. Immunity. 2016;44(5):989-1004.

35. Long AH, Haso WM, Shern JF, et al. 4-1BB costimulation ameliorates T cell exhaustion induced by tonic signaling of chimeric antigen receptors. Nat Med. 2015;21(6):581-590.

36. Han G, Chen G, Shen B, Li Y. Tim-3: an activation marker and activation limiter of innate immune cells. Front Immunol. 2013;4:449.

37. Ghermezi M, Li M, Vardanyan S, et al. Serum B-cell maturation antigen: a novel biomarker to predict outcomes for multiple myeloma patients. Haematologica. 2017;102(4):785-795.

38. Bal S, Sigler A, Chan A, et al. First Description of B cell maturation antigen expression in light chain amyloidosis. Blood. 2019;134(Suppl 1):S5452.

39. Guedan S, Calderon H, Posey AD, Jr., Maus MV. Engineering and design of chimeric antigen receptors. Mol Ther Methods Clin Dev. 2018;12:145-156.

40. Lindner SE, Johnson SM, Brown CE, Wang LD. Chimeric antigen receptor signaling: functional consequences and design implications. Sci Adv. 2020;6(21):eaaz3223.

41. Smith EL, Harrington K, Staehr M, et al. GPRC5D is a target for the immunotherapy of multiple myeloma with rationally designed CAR T cells. Sci Transl Med. 2019;11(485):eaau7746.

42. Ying Z, Huang XF, Xiang X, et al. A safe and potent anti-CD19 CAR T cell therapy. Nat Med. 2019;25(6):947-953.